Mechanism of Fluorescence and Conformational Changes of the Sarcoplasmic Calcium Binding Protein of the Sand Worm *Nereis diversicolor* upon Ca^{2+} or Mg^{2+} Binding

Alain Sillen,* Stefan Verheyden,* Lotte Delfosse,* Tania Braem,* Johan Robben,† Guido Volckaert,† and Yves Engelborghs*

*Laboratory of Biomolecular Dynamics; and †Laboratory of Gene Technology; Catholic University of Leuven, Leuven, Belgium

ABSTRACT The calcium-binding protein isolated from the sarcoplasm of the muscles of the sand worm *Nereis diversicolor* has four EF-hands and three active binding sites for Ca^{2+} or Mg^{2+}. *Nereis diversicolor* sarcoplasmic calcium-binding protein contains three tryptophan residues at positions 4, 57, and 170, respectively. The Wt protein shows a very limited fluorescence increase upon binding of Ca^{2+} or Mg^{2+}. Single-tryptophan-containing mutants were produced and purified. The fluorescence titrations of these mutants show a limited decrease of the affinity for calcium, but no alterations of the cooperativity. Upon adding calcium, *Trp*170 shows a strong fluorescence increase, *Trp*57 an extensive fluorescence decrease, and *Trp*4 shows no fluorescence change. Therefore mutant W4F/W170F is ideally suited to analyze the fluorescence titrations and to study the binding mechanism. Mutations of the calcium ligands at the *z*-position in the three binding sites show no effect at site I and a total loss of cooperativity at sites III and IV. The quenching of *Trp*57 upon calcium binding is dependent on the presence of arginine R25, but this residue is not just a simple dynamic quencher. The role of the salt bridge R25-D58 is also investigated.

INTRODUCTION

Conformational changes play an essential role in the function of proteins. A very sensitive way to study these conformational changes is monitoring the change in tryptophan fluorescence properties. Tryptophan is a naturally occurring fluorescent probe present in most proteins and is sensitive to its immediate environment. Therefore it can be used to study interesting regions in the protein that play an essential role in the conformational change of the protein as a whole. Conformational changes are usually induced by ligand binding and calcium binding is a particularly interesting case. In this work we studied the calcium binding protein isolated from the sarcoplasm of the muscles of the sand worm *Nereis diversicolor* (NSCP), which has 174 amino acids (Collins et al., 1988) and a relative molecular mass of 19,485. The three-dimensional x-ray structure (at 2 Å resolution) of Ca^{2+}-bound NSCP (Fig. 1) is described by Vijay-Kumar and Cook (1992) and the nuclear magnetic resonance (NMR) structure is described by Craescu et al. (1998). NSCP has four domains with the typical EF-hand (Kretsinger and Nockolds, 1973) Ca^{2+}-binding sequence, but only sites I, III, and IV can bind Ca^{2+} or Mg^{2+}. The protein has a compact structure with a central hydrophobic core of 20 amino acids, most of which are aromatic. The domains I and II form a pair by a back-to-back β-sheet just like the pair of III and IV. NSCP is mainly α-helical (58%) with eight helices (A–H). Initial Ca^{2+}-binding studies were analyzed in terms of three identical intrinsic binding constants of $1.7 \times 10^8\ M^{-1}$ at pH 7.5 and 25°C, whereas Mg^{2+} binding was found to be cooperative with intrinsic binding constants of 0.83, 2.6, and $15 \times 10^4\ M^{-1}$, respectively (Cox and Stein, 1981). Further conformational and microcalorimetry studies on the protein (Luan-Rilliet et al., 1992) and on isolated tryptic fragments lead to the proposal of a new sequential binding model starting at site I (Durussel et al., 1993). In this study we use site-directed mutagenesis instead of protein fragments to analyze the binding mechanism.

NSCP contains three tryptophan residues at positions 4, 57, and 170, respectively. These tryptophans are located at interesting positions in the protein. *Trp*4 is positioned at the beginning of helix A and is not involved in an EF-hand, but is close to helix D which makes the connection between domains II and III together with helix E. *Trp*57 is positioned at the second (inactive) domain with the indole group close to the binding site of the first domain. This makes W57 ideally located for observing the changes at the interdomain region between domains I and II upon binding of Ca^{2+} or Mg^{2+}. *Trp*170 is positioned at the end of the last helix H, but the indole group is located in the hydrophobic core in the center of the protein. Therefore W170 is ideally located for observing the general conformational change in the protein. Altogether, NSCP is an interesting model protein to study the conformational change upon ion binding—also because it has a high sequence similarity with other sarcoplasmic Ca^{2+}-binding proteins (Nakayama and Kretsinger, 1994), e.g., the sarcoplasmic calcium-binding proteins from shrimp, crayfish, and streptomyces. In proteins, tryptophan fluorescence displays a multiexponential decay originating from the different possible microconformations of tryptophan (Dahms et al., 1995; Sillen et al., 2000). Other models are also suggested to explain the existence of a multiexponential decay

Submitted December 6, 2002, and accepted for publication May 22, 2003.

Address reprint requests to Yves Engelborghs, Katholieke Universiteit Leuven, Celestijnenlaan 200D, B-3001 Leuven, Belgium. Tel.: 321-632-7160, Fax: 321-632-7982; E-mail: yves.engelborghs@fys.kuleuven.ac.be.

Johan Robben's present address is Biomedical Research Ctr., Limburg University Ctr., Universitaire Campus, B3590 Diepenbeek, Belgium.

0006-3495/03/09/1882/12 $2.00

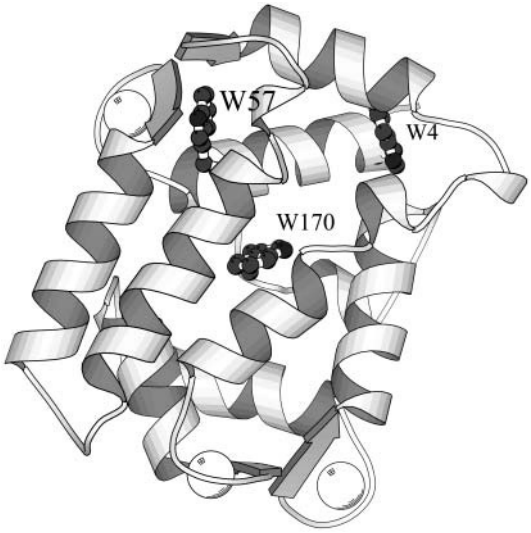

FIGURE 1 MOLSCRIPT representation of the x-ray structure of NSCP Ca^{2+}. The white spheres represent the calcium ions.

(Alcala et al., 1987; Van Gilst et al., 1994; Lakowicz, 2000). NSCP is also an interesting protein to gain more insight into protein fluorescence.

EXPERIMENTAL PROCEDURES

Materials

Isopropyl β-D-thiogalactoside (IPTG) was obtained from Promega (Madison, WI). $MgCl_2$ and EDTA were purchased from Janssen Chimica (Beerse, Belgium). $CaCl_2$ was obtained from Riedel de Haen (Seelze, Germany), GuHCl from Fluka (Buchs, Switzerland), and *n*-acetyltryptophanamide and EGTA were obtained from Sigma Chemical (St. Louis, MO). The buffer solution was 50 mM Tris·HCl at pH 7.5. The ionic strength of the solutions was always 0.2-M adjusted with KCl. All buffer reagents were of analytical grade and were obtained from Sigma, Janssen Chimica, ICN (Aurora, Ohio), or Fluka. All solutions were filtered through a 0.22-μm filter (Millipore, Billerica, MA) and were spectroscopically pure. All the restriction endonucleases and Klenow polymerase were obtained from either New England Biolabs (Beverly, MA) or Boehringer (Mannheim, Germany). The DNA purification kits were from Diagen (Düsseldorf, Germany).

Mutagenesis

The NSCP gene was transferred from the plasmid pNDner06 (Dekeyzer et al., 1994) into the plasmid pET22b(+) (Studier et al., 1990) resulting in pETNSCP (van Riel, 1997). In this plasmid the NSCP gene is under control of the strong T7 promoter. For expression of NSCP mutants, the plasmid pETNSCP was used, into which the NSCP mutant genes were constructed either by polymerase chain reaction or by cassette mutagenesis. Site-directed mutagenesis was performed according to Sambrook et al. (1989). The following oligonucleotides were used:

D27N:

5′-TAGATTCGAAGT**T**CATACGAGTGATAGCAC-3′

*Bst*BI

E115Q: 5′-GAGAC**C**AATACGGTATCTTCTTC-3′

E149Q: 5′-GTCTCTCGAG**C**AATTCGTTATCGCAG-3′

*Xho*I

The tryptophan mutations and R25D and D58R are described in Sillen et al. (2000).

Mutants were identified by restriction analysis and the mutated genes were entirely sequenced using the ABI PrismTM Big Dye Terminator Cycle Sequencing Ready Reaction system (PerkinElmer, Boston, MA).

Expression and purification

The *Escherichia coli* strain Bli5 (Bl21(DE3) + pDIA17) (Chang and Cohen, 1978; Studier and Moffat, 1986; Raleigh et al., 1988; Munier et al., 1991) was transformed by electroporation with the pETNSCP plasmids. Cells were then treated as described by Dekeyzer et al. (1994). The difference in negative charges between the Ca^{2+} and the apo states of the protein was used to purify NSCP. In a first step, NSCP, in the presence of Ca^{2+}, was isolated from the other cell proteins by anion exchange chromatography (DEAE, Fast-Flow, Pharmacia, Uppsala, Sweden). This was repeated, but with adjusting to 5 mM EGTA (apo conformation). In a last step, NSCP was purified on a Hiload Superdex 75 prepgrade 16/60 column (Pharmacia). All NSCP variants were ≥99% pure as judged by Coomassie-stained SDS gels. All the variants where stored with 2 mM $CaCl_2$. The apo form was made by adding EGTA and EDTA to a 10-mM concentration each. The Mg^{2+} form was made by adjusting the apo form solution to 20 mM $MgCl_2$.

Steady-state fluorescence

Steady-state fluorescence was measured with a SPEX spectrofluorometer (Fluorolog 1691, Spex Industries, Edison, NJ) with excitation and emission slits providing a bandpass of 7.2 and 3.6 nm, respectively. Spectra are corrected for the wavelength dependence of the emission monochromator and the photomultiplier and also by subtracting background intensities of the buffer solution. The cuvette holder was thermostated at 22°C. The excitation wavelength was 295 nm to ensure that the measured signal is only due to tryptophan fluorescence.

Ultraviolet absorption

Ultraviolet absorption was measured on a UVIKON Kontron 940 spectrophotometer (Kontron AG, Eching, Germany). The molar absorption coefficients at 295 nm are calculated by taking the ratio of the absorbance at 295 nm and at 280 nm, multiplied by the molar absorption coefficients at 280 nm, which was calculated according to the method of Mach et al. (1992).

Fluorescence lifetime data

Fluorescence lifetime data were determined as described previously (Sillen et al., 2000) using an automated multifrequency phase fluorometer. The instrument is similar to that described by Lakowicz et al. (1985), except for the use of a high-gain photomultiplier (Model H5023, Hamamatsu, Bridgewater, NJ) instead of a microchannel plate. The detection part is described by Vos et al. (1997). The excitation source consists of a mode-locked titanium-doped sapphire laser (Tsunami, Spectra-Physics, Mountain View, CA) pumped by a Beamlok 2080 Ar^+-ion laser (Model 2080, Spectra-Physics). After frequency-tripling (GWU, Spectra-Physics) the excitation wavelength is 295 nm. The fluorescence lifetime measurements are performed by measuring the phase-shift of the modulated emission at 50 frequencies ranging from 1.6 MHz to ~1 GHz. *N*-Acetyltryptophanamide (in water filtered by the Milli-Q system, Millipore) with a fluorescence lifetime of 3.059 ns or *p*-terphenyl in cyclohexane with a lifetime of 1.04 ns (Desie et al., 1986) both at 22°C was used as a reference fluorophore. The measured phase shifts, ϕ, at a modulation frequency, ω, of the exciting light are related to the fluorescence decay in the time domain $I(t)$,

$$I(t) = \sum_i a_i \exp\left(\frac{-t}{\tau_i}\right), \quad (1)$$

where a_i is the amplitude of the fluorescence signal of the component with lifetime τ_i, as described by Weber (1981).

Time-resolved anisotropy

Measuring the frequency-dependent phase difference between the parallel and perpendicular components of the modulated fluorescence revealed the rotational correlation times ϕ_i with their relative amplitudes ($\sum g_i = 1$), together with the initial anisotropy r_0 (anisotropy in the absence of depolarizing processes) by fitting the frequency transform of a multi-exponential anisotropy decay law (Weber, 1977),

$$r_{(t)} = r_0 \sum_i g_i \exp(-t/\phi_i), \tag{2}$$

where g_i are the amplitudes and ϕ_i the rotational correlation times. The analysis was performed assuming that each fluorescing species with lifetime τ_i has the same anisotropy function (Lakowicz et al., 1985). No indication for associative decay was found. The rotation angle of tryptophan was calculated according to Lipari and Szabo (1980) for free diffusion within a cone angle θ.

$$g_1 = \left[\frac{\cos\theta(1+\cos\theta)}{2}\right]^2. \tag{3}$$

Data analysis was performed using a nonlinear least-squares algorithm (Bevington, 1969). Several statistical techniques were used in the fitting procedure, as described by Clays et al. (1989). Measurements performed at different emission wavelengths were analyzed simultaneously with global analysis (GLOBALS Unlimited, University of Illinois, Urbana, IL) to increase the resolution of the lifetimes and the corresponding amplitudes (Beechem et al., 1983). Phase data were fitted using the modified Levenberg-Marquardt algorithm (More and Sorensen, 1983) assuming fluorescence lifetimes that are independent of the emission wavelength and a variable amplitude ratio. The lifetimes did not change across the different wavelengths.

Quantum yields were determined relative to tryptophan in water according to the method of Parker and Rees (1960), where the intensity is integrated over the wavelength region 300–450 nm, with the absorbance at 295 nm, and the quantum yield Q_{Trp} for tryptophan in water is taken as 0.14 (Kirby and Steiner, 1970).

Decay-associated spectra

Decay-associated spectra are constructed by multiplying the intensity fraction with the intensity of the emission spectra at the respective wavelength (Ross et al., 1981). A log-normal function (Burstein and Emelyanenko, 1996) is fitted to the associated intensities to obtain the decay-associated spectra.

The average radiative rate constant is calculated by dividing the quantum yield by a wavelength-independent amplitude average lifetime (Willis and Szabo, 1992; Sillen and Engelborghs, 1998). Each lifetime is integrated over the wavelength region 300–450 nm and then normalized (Sillen et al., 2000).

Calculation of the change in fluorescence intensity due to static and dynamic quenching and by a change in the population of microconformations

We suggested splitting the ratio of the quantum yield of different variants relative to a reference protein, e.g., Wt, into a factor (f_{kr}) representing the change in k_r, or homogenous static quenching, a factor (f_{PR}) reflecting heterogeneous static quenching or population reshuffling, and a factor (f_{DQ}) representing pure dynamic quenching (Sillen and Engelborghs, 1998; Sillen et al., 1999). The factor f_{PR} is affected by static quenching only if the static quenching is heterogeneous. If there is static quenching and an increase of the fluorescence due to population reshuffling, then f_{PR} is the minimum increasing factor of fluorescence intensity due to a change in the balance between microconformations.

EGTA titration

NSCP Wt and variants are excited at 295 nm, and the emission is measured at maximum emission wavelength (Ca^{2+} state). We use a quartz cuvette with stirrer (1-cm optical pathway, Hellma Benelux, Aartselaar, Belgium) that contains 1.2 ml of the protein solution. The protein concentration is 13 μM. This solution contains ~0.2 mM $CaCl_2$. The correct concentration of Ca^{2+} in the solution is determined by an atomic absorption spectrophotometer (Model 372, PerkinElmer).

First, the fluorescence is measured 60× during 1 min. Then a certain volume (2–10 μl) of a 250 or 500 mM EGTA solution is added, depending on the current free calcium concentration. After addition of EGTA, the solution is equilibrated for 3 min before the next measurement.

To calculate the concentration of Ca^{2+} present in the solution, we use the software program Chelator (Schoenmakers, 1992) that takes the concentration of EGTA, buffer, temperature, and ionic strength into account. During the titration the ionic strength increases, due to the addition of Na_2-H_2·EGTA, from the original value of 0.1 M to 0.106 M. Between Ca^{2+} concentrations it decreases from 0.2 mM to 10^{-8}M and the ionic strength increases to 0.16 M when Ca^{2+} is further decreased to 10^{-9} M. Calcium Green-1 indicator (Molecular Probes, Eugene, OR) is a fluorescent indicator used to check the titration procedure and the calculations made by Chelator. Calcium Green-1 indicator has a single binding site for Ca^{2+}. The indicator is excited at 488 nm and the fluorescence is measured at 533 nm. Upon binding of Ca^{2+} the fluorescence increases. The indicator is titrated the same way as the protein samples and the correct binding constant of 5.2×10^6 M^{-1} was obtained.

Quin 2 titration

Quin 2 titrations are done according to Linse et al. (1991). Quin 2 separately and Quin 2 (25 μM), together with NSCP (10 μM), are titrated with Ca^{2+} by monitoring the absorption of Quin 2 at 263 nm. First, the exact concentration of Quin 2 is determined by titration with Ca^{2+} and the dissociation constant is 60 nM (Tsien and Pozzan, 1989) at the ionic strength of 0.10 M. During the titration the ionic strength increases to 0.11 M due to the addition of Ca^{2+}. The absorption in the absence of Ca^{2+} (OD_{max}) is determined by measuring Quin 2 with 10 mM EGTA. Then Quin 2, together with NSCP, are titrated with Ca^{2+}. The exact concentration of NSCP is determined by measuring the absorption at 280 nm. The absorption of the Ca^{2+} free system (OD_{max}) is determined by measuring Quin 2, NSCP, and 10 mM EGTA. The amount of bound Ca^{2+} is calculated from the OD_{max} and the absorption at excess Ca^{2+}. From this it is possible to calculate the fractional saturation of NSCP with Ca^{2+}.

Fitting

Curve fitting of the fluorescence titration curves is done with a nonlinear least-squares fitting program (SigmaPlot-5, SPSS, Chicago, IL). Attempts were made to fit the whole titration curve to the full Adair equation

$$F = \frac{F_0 + \sum_{i=1}^{i=3} F_i \varphi_i [Ca^{2+}]^i}{\sum_{i=1}^{i=3} \varphi_i [Ca^{2+}]^i}, \tag{4}$$

where seven fitting parameters are necessary (i.e., φ_I is the Adair coefficient, and F_i is the relative fluorescence of the species NSCP). Ca_i was not acceptable, because the parameters obtained displayed a strong dependency

(parameter d), indicating that too many parameters are being extracted from the data set. Therefore, a simplified equation assuming variable cooperativity was used,

$$F = \frac{F_0 + F_3(K[Ca^{2+}])^n}{1 + (K[Ca^{2+}])^n}, \quad (5)$$

with n the Hill coefficient (here assumed to be constant during the titration) and K the average association constant for the three sites.

This equation, however, cannot be used to fit the titration curve of the Wt because in Wt the fluorescence change is biphasic, i.e., a fluorescence decrease is followed by an increase. The biphasic curve could be fitted with the following equation:

$$F = \frac{F_0 + F_1\varphi_1[Ca] + F_3\varphi_3[Ca]^3}{1 + \varphi_1[Ca] + \varphi_3[Ca]^3}. \quad (6)$$

We also used Quin titrations in this case and analyzed them with the Hill equation. Our results and numerical simulations show that the Hill coefficient obtained from direct binding studies can be substantially lower (1.8×) than those obtained from protein fluorescence titrations, due to the nonlinear relation between protein fluorescence and calcium binding.

RESULTS

Fluorescence spectra and quantum yields of the NSCP variants

Analysis of the fluorescence spectra (Figs. 3 and 4) and the quantum yields (Table 1) of NSCP and the different mutants that were measured in Ca^{2+}-bound, Mg^{2+}-bound, and apo states, reveals that the quantum yield of Wt decreases only slightly in the following order of $Ca^{2+} > Mg^{2+} >$ apo. The quantum yield of Wt is 0.14, a typical value for free tryptophan. The two tryptophan residues that show a large fluorescence change upon Ca^{2+} removal are W57 and W170. This large change is not observed in Wt because the changes in the two tryptophans have opposite signs; the quantum yield of W170 increases from 0.09 to 0.14, whereas the quantum yield of W57 decreases from 0.14 to 0.03 upon the binding of Ca^{2+}. The fluorescence of W4 increases only slightly upon binding of Ca^{2+}. The quantum yield of W4 varies between 0.21 and 0.24 for all states, which is a rather high value. The fluorescence of W57 is also strongly influenced by the salt bridge R25-D58 in the environment of W57. It is interesting to note that the molar absorption coefficients of individual tryptophans at 295 nm can vary between 2338 and 3194, whereas the molar absorption coefficient at 280 nm is much more constrained (Mach et al., 1992).

TABLE 1 Molar absorption coefficients, quantum yield, average lifetime, and radiative rate constant of NSCP and variants

	ε_{295} ($M^{-1}cm^{-1}$)	Q	$\langle\tau\rangle$ (ns)	$\langle kr\rangle$ (ns^{-1})	λ_{max} (nm)
		Wt			
Ca	7923 ± 178	0.143 ± 0.02	2.92	0.049	338
Mg	6882 ± 98	0.141 ± 0.01	2.7	0.052	339
Apo	8678 ± 177	0.14 ± 0.01	2.88	0.049	338
		W57F/W170F			
Ca	2980 ± 71	0.226 ± 0.02	4.8	0.047	339
Mg	2688 ± 92	0.240 ± 0.03	4.6	0.052	339
Apo	2890 ± 148	0.21 ± 0.03	4.8	0.044	338
		W4F/W57F			
Ca	2978 ± 215	0.135 ± 0.001	3.6	0.037	338
Mg	2708 ± 234	0.121 ± 0.002	3.96	0.031	341
Apo	2447 ± 133	0.092 ± 0.007	2.9	0.032	350
		W4F/W170F			
Ca	2338 ± 198	0.033 ± 0.001	0.61	0.054	317
Mg	2501 ± 321	0.032 ± 0.001	0.59	0.054	324
apo	2957 ± 152	0.14 ± 0.01	3	0.048	330
		W4F/W170F/R25D			
Ca	2878 ± 398	0.10 ± 0.02	2.2	0.046	336
Mg	2984 ± 473	0.09 ± 0.01	2	0.046	336
apo	3142 ± 357	0.13 ± 0.06	2.8	0.046	345
		W4F/W170F/R25D/D58R			
Ca	2873 ± 45	0.12 ± 0.01	2.5	0.048	325
Mg	2673 ± 47	0.08 ± 0.01	1.5	0.052	323
apo	3194 ± 38	0.18 ± 0.01	3.4	0.052	328

Time-resolved fluorescence parameters

The measurements were performed at emission wavelengths ranging from 320 to 380 nm in 10-nm intervals. A typical measurement is shown in Fig. 2. A single- or double-exponential fit to the phase data yielded unacceptably high values of χ_R^2 and a significant nonrandomness in the autocorrelation function of the weighted residuals as

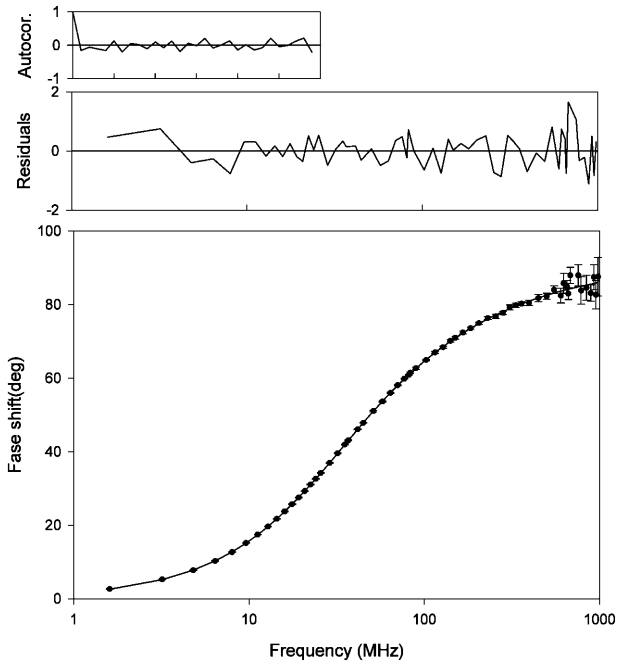

FIGURE 2 Typical phase measurement of NSCP W4F/W170F/R25D/D58R apo and graphical tests incorporated in the data analysis (spreading and autocorrelation analysis of the residuals). Fit to four exponentials.

a function of the frequency. Best fit with lowest χ_R^2 and no systematic deviations in the autocorrelation function of the weighted residuals is obtained with a triple- or quadruple-exponential function. To improve the recovery of the decay parameters, a global analysis of all the phase measurements at the different wavelengths was performed. The results of this global fit are summarized in Table 2. The decay-associated spectra are shown in Figs. 3 and 4.

Anisotropy decay parameters

Time-resolved anisotropy measurements are obtained from the frequency-dependent phase angle difference between the parallel and perpendicular components of the modulated fluorescence emission. Best fit with χ_R^2 near unity and no systematic deviations in the weighted residuals is obtained with a double-exponential fit resulting in two rotational correlation times. The results of the fit are summarized in Table 3. The long rotational correlation time can be associated with the overall rotation of NSCP, whereas the short rotation correlation time can be associated with the local motion of the tryptophan (Lakowicz, 1999). The apparent time zero anisotropy r_0 for tryptophan and tryptophan derivatives is ~0.19 at 295 nm (Valeur and Weber, 1977; Lakowicz et al., 1983), usually interpreted as due to the presence of ^1L_a and ^1L_b absorption bands (Callis, 1997; Ruggiero et al., 1990). This is also the case for most of the NSCP variants.

Fluorescence and EGTA titration of NSCP

Although the fluorescence titration curves of the single-tryptophan-containing mutants show big changes in fluorescence intensities, we could not fit them to the full Adair equation (Eq. 4) because the fitting program (SigmaPlot) signals that the parameters are strongly interdependent, indicating that one is forced to use a simpler equation. We therefore switched to the Hill equation (Eq. 5) with essentially only two parameters (K and n), since F_0 and F_3 are the extremes of the titration curves.

However, titration of Ca^{2+} Wt with EGTA gives rise to a biphasic fluorescence change (Fig. 5). Starting from the high Ca^{2+} concentrations, first a decrease in fluorescence, and subsequently an increase, is observed. Such a biphasic curve cannot be fitted with a simple Hill equation. We performed Quin titrations as an alternative method to monitor the binding of Ca^{2+} to NSCP Wt by measuring the absorption change of Quin 2 in the presence of NSCP Wt with Ca^{2+}. From this the association constants was determined to be $(9.8 \pm 0.4) \times 10^7$ (M^{-1}) and the Hill coefficients was 1.6 ± 0.2. It should be noted that this Hill coefficient is an underestimation of the one determined by protein fluorescence changes by as much as a factor of 1.8

TABLE 2 Lifetimes (τ), wavelength independent amplitude fraction (α), and χ_R^2 as obtained by global analysis of the fluorescence decay of NSCP and its variants in the Ca^{2+}, Mg^{2+}, and apo states

Wt	α_1	τ_1(ns)	α_2	τ_2 (ns)	α_3	τ_3 (ns)	α_4	τ_4 (ns)	χ_R^2
Ca	0.31 ± 0.03	0.21 ± 0.04	0.14 ± 0.02	1.3 ± 0.2	0.55 ± 0.02	4.8 ± 0.2	0.002 ± 0.04	12 ± 9	2.8
Mg	0.32 ± 0.01	0.32 ± 0.1	0.10 ± 0.002	0.99 ± 0.4	0.28 ± 0.09	3.2 ± 0.7	0.29 ± 0.5	5.6 ± 1	2
apo	0.2 ± 0.2	0.42 ± 0.2	0.36 ± 0.08	1.9 ± 0.9	0.42 ± 0.07	4.6 ± 0.9	0.013 ± 0.008	11 ± 4	2.2
					W57F/W170F				
Ca	0.029 ± 0.005	0.42 ± 0.05	0.20 ± 0.03	3.2 ± 0.2	0.8 ± 0.4	5.2 ± 0.1			1.3
Mg	0.068 ± 0.003	0.22 ± 0.03	0.26 ± 0.02	3.48 ± 0.06	0.68 ± 0.3	5.45 ± 0.09			1.7
apo	0.050 ± 0.005	0.78 ± 0.3	0.29 ± 0.09	3.75 ± 0.2	0.66 ± 0.4	5.56 ± 0.2			2.3
					W4F/W57F				
Ca	0.15 ± 0.04	0.61 ± 0.2	0.34 ± 0.04	2.7 ± 0.5	0.51 ± 0.06	5.1 ± 0.3			3.1
Mg	0.116 ± 0.05	0.767 ± 0.2	0.303 ± 0.04	2.745 ± 0.5	0.581 ± 0.06	5.227 ± 0.226			2.3
apo	0.24 ± 0.02	0.63 ± 0.05	0.54 ± 0.02	2.77 ± 0.1	0.222 ± 0.03	5.63 ± 0.2			1
					W4F/W170F				
Ca	0.66 ± 0.06	0.19 ± 0.08	0.23 ± 0.03	0.66 ± 0.20	0.09 ± 0.01	2.4 ± 0.3	0.02 ± 0.07	5.8 ± 0.3	3
Mg	0.58 ± 0.07	0.14 ± 0.04	0.29 ± 0.05	0.52 ± 0.06	0.11 ± 0.01	2.1 ± 0.2	0.025 ± 0.09	5.1 ± 0.4	2.3
apo	0.20 ± 0.02	0.27 ± 0.07	0.24 ± 0.03	1.4 ± 0.2	0.46 ± 0.03	4.0 ± 0.3	0.097 ± 0.05	7.2 ± 0.7	2.1
					W4F/W170F/R25D				
Ca	–	–	0.44 ± 0.02	0.42 ± 0.03	0.35 ± 0.02	2.4 ± 0.1	0.21 ± 0.02	5.7 ± 0.2	2.1
Mg	–	–	0.52 ± 0.02	0.43 ± 0.02	0.30 ± 0.02	2.4 ± 0.2	0.18 ± 0.02	5.7 ± 0.2	2.4
apo	–	–	0.26 ± 0.02	0.42 ± 0.05	0.46 ± 0.02	2.49 ± 0.14	0.28 ± 0.03	5.5 ± 0.2	2.1
					W4F/W170F/R25D/D58R				
Ca	0.21 ± 0.08	0.4 ± 0.1	0.27 ± 0.05	1.1 ± 0.3	0.45 ± 0.02	3.6 ± 0.1	0.07 ± 0.06	6.7 ± 0.7	0.8
Mg	0.45 ± 0.04	0.23 ± 0.03	0.26 ± 0.03	0.99 ± 0.2	0.25 ± 0.01	3.6 ± 0.3	0.04 ± 0.02	7.1 ± 0.8	1.5
apo	0.13 ± 0.2	0.5 ± 0.2	0.31 ± 0.1	2.0 ± 0.5	0.55 ± 0.1	4.7 ± 0.5	0.02 ± 0.1	9 ± 4	1

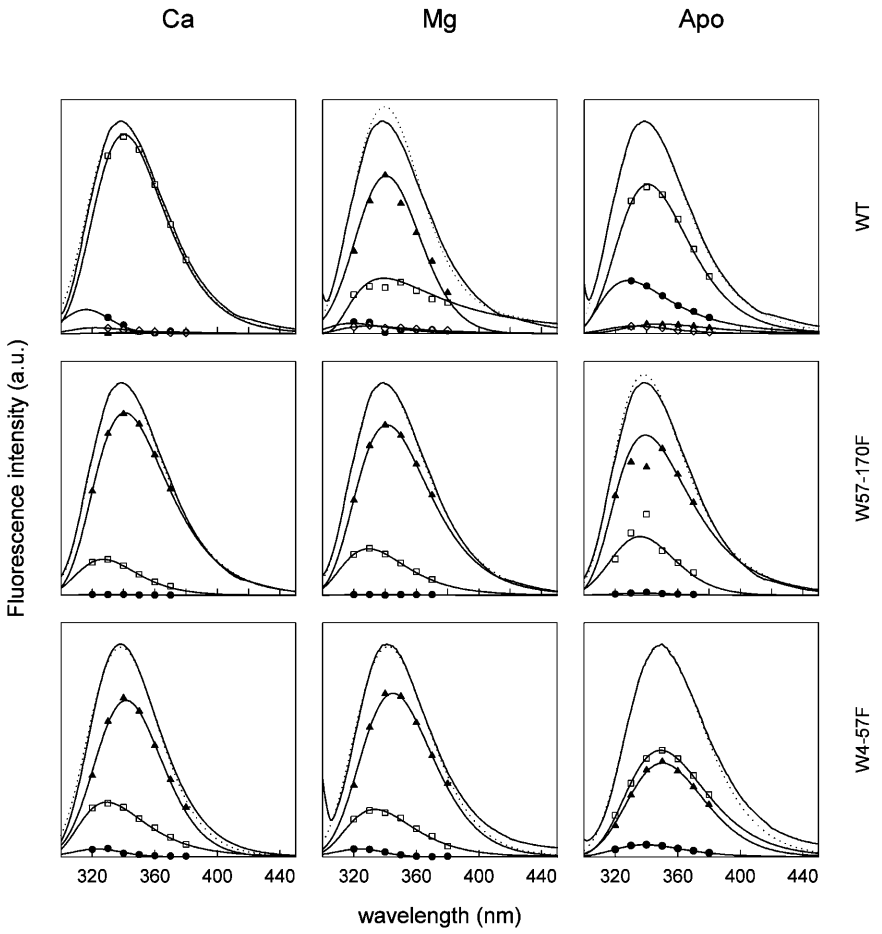

FIGURE 3 Normalized decay-associated spectra (*DAS*) of Wt, W57F/W170F, and W4F/W57F in the Ca^{2+}, Mg^{2+}, and apo states. Spectra are from 300 nm to 450 nm. ▲, longest lifetime; □, second longest lifetime; ●, middle lifetime; ◇, smallest lifetime; –, measured emission spectra; and . . ., sum of the decay-associated spectra.

(shown by numerical simulations) due to the nonlinear relation between saturation and conformation.

The fluorescence titration of Wt protein could also be fitted with a simplified Adair equation (Eq. 6) and the following parameters were obtained: $F_0 = 2.13 \pm 0.02$, $F_1 = 1.91 \pm 0.03$, $F_3 = 2.27 \pm 0.01$ (all $\times 10^5$ in arbitrary units), $\varphi_1 = (1.3 \pm 0.5) \times 10^9\ M^{-1}$, and $\langle \varphi_3 \rangle^{1/3} = (2.9 \pm 0.2) \times 10^8\ M^{-1}$. However, we do not trust the first binding constant, because at calcium concentrations $<10^{-9}$ M the ionic strength of the solution increases too much. Fitting the titrations of W57 and W170 (Fig. 6 and Table 4) and comparing with Wt reveals that mutating two tryptophans into Phe changes the association constant of Ca^{2+} to NSCP to somewhat lower values. The association constants and Hill coefficients are summarized in Table 4. But the mutations have no effect on the cooperativity of the binding because the Hill coefficient of Wt and W4F/W57F are approximately the same, and is only slightly lower for the W4F/W170F variant ($n = 2.6$) (Table 4), taking into account the effect of the factor 1.8 between the Hill coefficient obtained from fluorescence titrations and from direct binding studies. Mutating calcium ligands in the ion-binding loop of domain I has only little effect on the association constants and Hill coefficients (Table 4). Mutations in domains III and IV, however, lower the association constants and reduce the Hill coefficients to 1. To check whether the mutations of tryptophan have an influence on the fluorescence of the remaining tryptophan residues, we calculated the fluorescence intensity of the different tryptophans and compared the addition of the intensities with the fluorescence intensity of Wt (Table 5). In all ion-binding states of NSCP, the sum of the fluorescence intensity approximates the intensity of Wt very closely.

DISCUSSION

EGTA and Quin 2 titration of NSCP

To determine the binding mechanism of Ca^{2+} to NSCP, Ca^{2+}-bound NSCP and mutants were titrated with EGTA or, as alternative method, Quin 2 and NSCP with Ca^{2+}. The association constant and Hill coefficients were determined (Table 4 and Figs. 5 and 6). Comparing Wt with W4F/W170F and W4F/W57F shows that replacing the tryptophans lowers the affinity for calcium ions but has no effect on the cooperativity of binding. The Hill coefficients determined by

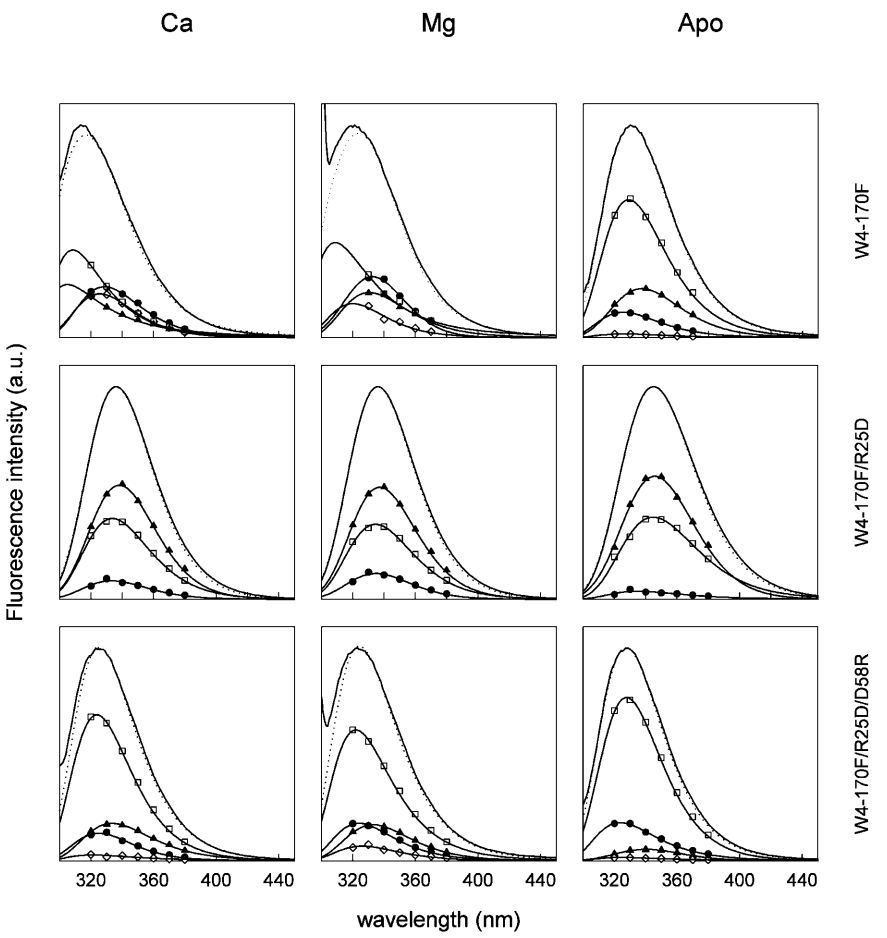

FIGURE 4 Normalized decay-associated spectra (*DAS*) of W4F/W170F, W4F/W170F/R25D, and W4F/W170F/R25D/D58R in the Ca^{2+}, Mg^{2+}, and apo states. Spectra are from 300 nm to 450 nm. ▲, longest lifetime; □, second longest lifetime; ●, middle lifetime; ◇, smallest lifetime; –, measured emission spectra; and . . ., sum of the decay-associated spectra.

monitoring the fluorescence change are 1.8× bigger than the value determined by Quin 2 titration due to the non-linearity of the fluorescence change with the Ca^{2+} binding which can be confirmed by simple simulations (Engelborghs et al., 1990). Changing the calcium binding residue (*z*-position) in domain I has only a small influence on Ca^{2+} binding, although changing the residues (*z*-positions) in domains III and IV, on the other hand, has a large influence on the Ca^{2+} binding, in that the average affinity is not much influenced but the cooperativity is totally lost. Mutation of the *z*-position in site I (D20N) has very little effect on the calcium-binding properties (data not shown). Mutation at the *z*-position (D108N) in site III has a similar effect as the mutation at *z* in site III: loss of cooperativity, but little effect on the overall binding constant (data not shown). A sequential binding mechanism was observed for recoverin (Permyakov et al., 2000) and calmodulin (Haiech and Kilhoffer, 2000). But in the case of recoverin the binding was totally lost by a mutation in the first binding site. Here it is clear that binding at sites III or IV both cause a cooperative transition, and that the ligands at *z*-position are crucial probably by pulling the α-helices together to form the EF-hand.

Fluorescence properties of individual tryptophan residues

W4

*Trp*4 is positioned at the beginning of the helix A and is not involved in a EF-hand, but is close to helix D which, together with helix E, makes the connection between domains II and III. Quantum yield, average lifetime, decay-associated spectra, lifetimes, anisotropy data. and quenching analysis reveal that there is only a minor change in the environment of W4 upon addition of Ca^{2+} or Mg^{2+} (Table 6). The high quantum yield is the result of the high population (80%) of the long lifetime (5.2 ns). This mutant protein was not further studied.

W170

*Trp*170 is positioned at the end of helix H, but the indole group is located in the hydrophobic core in the center of the protein. This makes W170 ideally located for observing the general conformational change in the protein. Indeed, upon changing from the Ca^{2+} state to the Mg^{2+} state there is a decrease of the quantum yield of 10%, and from the Ca^{2+}

TABLE 3 Anisotropy parameters of NSCP and variants in the different states

		r_0	g_1	ϕ_1 (ns)	ϕ_2 (ns)	χ_R^2	θ
W57F/W170F	Ca	0.20 ± 0.01	0.91 ± 0.01	10.6 ± 0.8	0.78 ± 0.3	0.6	14
	Mg	0.21 ± 0.03	0.9 ± 0.2	11.4 ± 3	0.45 ± 0.4	1.6	16
	apo	0.20 ± 0.01	0.89 ± 0.02	10.9 ± 0.7	0.5 ± 0.2	0.7	15
W4F/W57F	Ca	0.216 ± 0.001	0.74 ± 0.02	7.8 ± 1	0.76 ± 0.2	0.7	25
	Mg	0.22 ± 0.01	0.68 ± 0.02	7.3 ± 1	0.68 ± 0.2	0.7	28
	apo	0.17 ± 0.02	0.54 ± 0.03	9.5 ± 5	0.67 ± 0.1	1.2	35
W4F/W170F	Ca	0.3 ± 0.1	0.89 ± 0.02	15 ± 7	0.68 ± 0.4	1.3	15
	Mg	0.22 ± 0.04	0.78 ± 0.02	10.8 ± 5	0.75 ± 0.2	0.9	22
	apo	0.15 ± 0.02	0.71 ± 0.03	17.9 ± 5	0.54 ± 0.09	2.5	26
W4F/W170F/R25D	Ca	0.19 ± 0.01	0.85 ± 0.02	9.1 ± 0.1	0.55 ± 0.2	0.6	18
	Mg	0.19 ± 0.02	0.82 ± 0.02	10.1 ± 2	0.63 ± 0.2	1.3	20
	apo	0.18 ± 0.01	0.69 ± 0.02	6.1 ± 0.9	0.46 ± 0.7	1.1	27
W4-170F/R25D/D58R	Ca	0.18 ± 0.02	0.81 ± 0.05	9.6 ± 1.5	0.18 ± 0.3	1.5	21
	Mg	0.20 ± 0.02	0.88 ± 0.04	10.9 ± 1.6	0.24 ± 0.2	1.3	16
	apo	0.19 ± 0.02	0.86 ± 0.01	14.2 ± 3	0.71 ± 0.2	1.2	17

to the apo state there is a decrease of 32% (Table 6). This effect originates in a decrease in the measured radiative rate constant and additionally for the apo state in a higher population of the short and middle lifetime at the expense of the longest lifetime (population reshuffling). The x-ray structure reveals that W170 is totally buried. It has a wavelength of maximum intensity (λ_{max}) of 338 nm in the Ca^{2+} state. This is considered to be typical for tryptophan residues in an environment that is highly hydrophobic but also with water molecules with low mobility bound to the protein matrix (Burstein, 1983; Eftink, 1990). In the apo state, λ_{max} shifts to 350 nm, which is characteristic for solvent-accessible tryptophans. This indicates that, although W170 is in the core of NSCP in the Ca^{2+} state, upon changing to the apo state the core opens and water can penetrate resulting in a partially denatured structure. This is confirmed by FTIR measurements: the percentage of α-helix drops in the apo state by 14% compared to the Ca^{2+} state, whereas the unordered structure rises from 26% to 38% (van Riel, 1997) and this is also confirmed by NMR and circular dichroism measurements (Christova et al., 2000; Prêcheur et al., 1996; Cox and Stein, 1981). Also the rotational correlation time associated with the rotation of the whole protein and the rotation angle θ of W170 and W57 increases in the apo state (Table 3). The hydrophobic core of NSCP consists of mainly Phe and Tyr residues. Three of these hydrophobic core residues (F28, Y116, and F150) are in direct contact with the EF-hand structure and they are always the immediate neighbor of the amino acid responsible for the complexation of the ions at *z*-position in all three sites. These amino acids are conserved in most sarcoplasmic calcium-binding proteins (Collins et al., 1988). Consequently, removal of Ca^{2+} or Mg^{2+} destabilizes the hydrophobic core of NSCP.

W57

*Trp*57 is positioned at the second inactive domain with the indole group close to the binding site of the first domain.

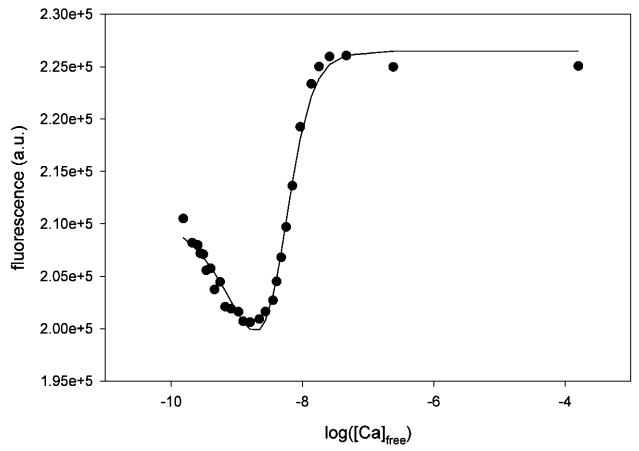

FIGURE 5 Fluorescence titration with EGTA of NSCP Wt containing 0.2 mM Ca^{2+}. Fluorescence is measured at 338 nm. *Continuous line* is the best fit using Eq. 6.

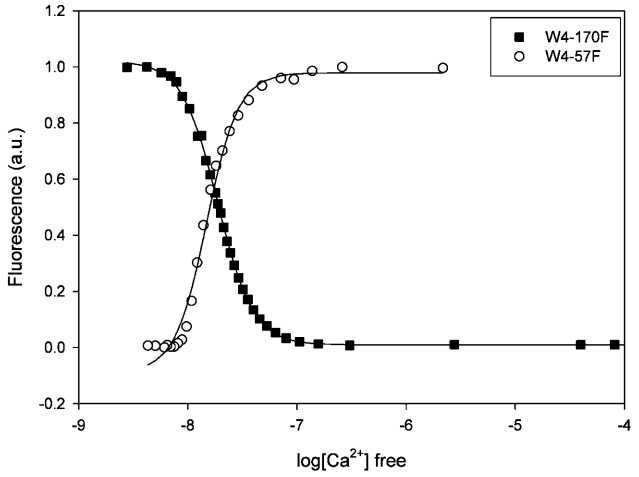

FIGURE 6 Normalized fluorescence titration with EGTA of NSCP mutants containing 0.2 mM Ca^{2+}. Fluorescence is measured at 338 nm for W170 and at 317 nm for W57. *Continuous line* is the best fit using Eq. 5.

TABLE 4 Quenching analysis

		kr/kr_0	f_{DQ}	f_{PR}	Q/Q_0
Wt	Ca→Mg	1.0547	0.542	1.7248	0.986
	Ca→apo	1.0025	1.06	0.9213	0.979
W57F/W170F	Ca→Mg	1.1047	1.0521	0.9136	1.0619
	Ca→apo	0.9323	1.0948	0.9104	0.9292
W4F/W57F	Ca→Mg	0.8177	1.0274	1.0669	0.8963
	Ca→apo	0.8494	1.0586	0.758	0.6815
W4F/W170F	Ca→Mg	1.0004	0.831	1.1664	0.9697
	Ca→apo	0.8826	1.5719	3.0581	4.2424
W4F/W170F/R25D	Ca→Mg	1.0152	1.0026	0.8841	0.9
	Ca→apo	1.0335	0.9948	1.2644	1.3
W4F/W170F/R25D/D58R	Ca→Mg	1.0659	0.9455	0.6615	0.6667
	Ca→apo	1.0739	1.3761	1.015	1.5
Ca	W57→R25D	0.8309	0.9461	3.8549	3.0303
	W57→D58R	0.8969	1.4494	2.7973	3.6364
Mg	W57→R25D	0.8432	1.0832	3.0794	2.8125
	W57→D58R	0.9556	1.6662	1.5702	2.5
Apo	W57→R25D	0.973	0.6622	1.4411	0.9286
	W57→D58R	1.0913	1.2264	0.9606	1.2857

kr/kr_0, quenching due to the change in apparent radiative rate constant; f_{DQ}, dynamic quenching; and f_{PR}, population reshuffling.

This makes W57 ideally located for observing the changes at the interdomain region of domains I and II upon binding of Ca^{2+} or Mg^{2+}. Upon binding of Ca^{2+} or Mg^{2+}, there is a fluorescence intensity decrease with a factor of 0.76 and 0.77, respectively. This decrease is largely caused by the higher population of the two lowest lifetimes—together, 89%—and is only to a limited extent due to direct dynamic quenching (Table 6). The different lifetimes of W57 have been explained on the basis of microstates of tryptophan (Sillen et al., 2000). The rotational correlation time of the whole protein and the rotation angle θ of W57 increases in the apo form, whereas the rotational correlation time of W57 itself decreases, indicating a more flexible environment of W57 in the apo form.

The λ_{max} of W57 in the Ca^{2+} state is very blue-shifted (317 nm), a phenomenon that could be due to the electromagnetic field over the tryptophan (Vivian and Callis, 2001).

TABLE 5 Association constant (*Ka*) and Hill coefficient (*n*) of NSCP variants

NSCP Variant	*Ka* (M^{-1})	*n*
Wt	$(9.8 \pm 0.2) \times 10^7$*	1.6 ± 0.2*
W4F/W57F	$(6.1 \pm 0.2) \times 10^7$	3.0 ± 0.3
W4F/W170F	$(5.32 \pm 0.04) \times 10^7$	2.65 ± 0.04
W4F/W170F/D27N (domain I)	$(3.5 \pm 0.1) \times 10^7$	2.6 ± 0.2
W4F/W170F/E115Q (domain III)	$(2.82 \pm 0.03) \times 10^7$	1.24 ± 0.01
W4F/W170F/E149Q (domain IV)	$(6.35 \pm 0.6) \times 10^6$	0.97 ± 0.09

*Constants obtained from Quin titrations; all other constants obtained from fluorescence titrations. The *n* obtained from Quin titrations can be substantially smaller than that from the fluorescence titration (see text).

Role of arginine R25

Although arginine is not found to be among the solution quenchers (Chen and Barkley, 1998), it is often observed as being a dynamic quencher of protein fluorescence (Clark et al., 1996; Christiaens et al., 2002) when arginine is very close to the aromatic ring of Trp. Studying the x-ray structure of NSCP, however, shows that the guanidinium moiety of R25 is not in contact with the aromatic rings of W57. Moreover, a detailed analysis of the quenching parameters (Table 6) indicates that the fluorescence change upon mutation R25D is largely due to population reshuffling (f_{PR}).

Influence of the salt bridge R25-D58 on the fluorescence properties of W57

*Trp*57 is located near the salt bridge R25-D58. This salt bridge connects the binding site of domain I with domain II. R25 is located adjacent to the amino acid responsible for the *x*-binding coordinate of the metal, and D58 is located in helix C. A similar situation exists in the two other domains of III and IV, where R113 is located just next to the amino acid responsible for the *x*-binding coordinate of the metal and forms a salt bridge with D135 located in helix G, and is in

TABLE 6 Fluorescence intensities $I(Q_\varepsilon)$ of the tryptophans in NSCP

I (M^{-1} cm^{-1})	Ca^{2+}	Mg^{2+}	Apo
W4	673	645	606
W57	77	80	413
W170	402	328	225
Sum	1153	1053	1246
Wt	1133	970	1214

close contact with binding site IV (9A from the Ca^{2+}). To investigate the influence of the salt bridge R25-D58 on the fluorescence of W57 and to investigate its function in the conformational change upon binding of the ions, two additional mutations were made—i.e., R25D, which breaks the salt bridge; and R25D/D58R, which potentially switches the orientation of the salt bridge.

W4F/W170F/R25D

Upon breaking of the salt bridge, the two lower lifetimes of the Ca^{2+} state converge to their arithmetic mean while the two longer lifetimes remain identical. The fluorescence lifetimes of the Ca^{2+}, Mg^{2+}, or apo forms are the same; only the amplitude fractions depend upon the binding of an ion. The apo state has a higher fluorescence intensity due to a higher population of the two longer lifetimes. The λ_{max} shifts ~10 nm to the red in changing from the Ca^{2+} state to the apo state in both W4F/W170F and W4F/W170F/R25D. This indicates that W57 is more solvent-accessible in the apo state.

There is a strong red-shift in all forms upon removing the salt bridge, indicating the existence of the salt bridge even in the apo form. Additionally, there is still a red-shift upon removing the Ca^{2+} ions from the binding site. The calcium binding site on its own is not able to create the fully shielded state of the W57. The intact salt bridge is partially responsible for this.

W4F/W170F/R25D/D58R

This mutation can potentially restore the salt bridge (but with opposite orientation, although we have no experimental evidence that it actually does so). This mutation has the effect that Ca^{2+} binding changes the amplitude fractions but keeps the lifetimes similar to those of the Wt apo state. Thus the lifetimes of W57 are Wt-apo-like in this mutant and the binding site is only affecting the population of the different micro conformations. The λ_{max} shifts only 3 nm to the red upon removal of Ca^{2+}, indicating a more similar solvent accessibility in the vicinity of W57 in comparison with W4F/W170F. Also in this variant all the lifetimes of the apo state are longer. Arginine is thus necessary for the longer fluorescence lifetimes and this elongation of the lifetimes is stronger in the apo state (Table 6). In the variant W4F/W170F, R25 interacts differently in the metal-bound state than in the metal-free state, resulting in a different conformation around W57 between the two states.

CONCLUSION

The x-ray structure determination reveals that the Ca^{2+} binding loop I is anchored to the rest of the protein by residues I15, R25, and F28. This Ca^{2+} binding loop is also connected by hydrogen bonds between the β-sheet of loop I to the β-sheet of the inactive loop II. The wavelength of maximum emission of W57 shifts from 317 nm to 330 nm in going from the Ca^{2+} state to the apo state, indicating a more solvent-accessible conformation. Also the anisotropy measurements reveal that W57 becomes more flexible in the apo state. Thus, one or more of the anchors has loosened or disappeared in the apo state. Upon removal of the salt bridge R25-D58, the wavelength of maximum emission of the holoform shifts from 317 nm to 336 nm and also the anisotropy data indicate a more flexible W57. In the apo state the wavelength of maximum emission shifts even further to 345 nm, indicating that W57 becomes very solvent-accessible. This proves that the salt bridge is still important even in the apo state of the W4F/W170F variant. Other interactions are therefore responsible for the formation of the holostate, e.g., the two amino acids I15 and F28, or other hydrogen bonds. These two amino acids are anchored in the hydrophobic core of NSCP. The wavelength of maximum emission of W170 shifts from 338 nm in the Ca^{2+} state to 350 nm in the apo state. This wavelength of maximum emission is the same as that of free tryptophan in solution. This indicates a large change in the hydrophobic core of NSCP. This supports the conclusion about the I15 and F28 anchors.

EGTA titration of the Wt and mutants and the Quin 2 titration of Wt reveals that cooperative binding occurs at domains III and IV probably due to the formation of the β-sheet that connects the two domains and that domain I behaves more as an independent site. The Hill coefficient, which is a measure for cooperativity, is ~2, indicating that there is cooperativity (although there is no real full cooperativity; $n = 3$). Both W57 and W170 are sensitive to the full conformational change due to ion binding (Fig. 5).

The behavior of the individual tryptophan residues (W57 and W170) is in agreement with the studies on tryptic fragments of NSCP done by Durussel et al. (1993). The N-terminal peptide (1–80) showed a single binding site with a $Ka = 3.1 \times 10^5\ M^{-1}$ and a fluorescence decrease upon calcium binding; the C-terminal peptide (90–174) showed two binding sites with $Ka = 3.2 \times 10^4\ M^{-1}$ and a fluorescence increase upon calcium binding. Combining this information with the biphasic behavior of the Wt protein it is tempting to assume a sequential-binding mechanism with initial binding at site I and then with strong cooperativity at sites III and IV. This sequence also explains that lowering the affinity at sites III and IV shows up as a decreased cooperativity, although the same mutation at site I does not influence the overall transition. This cooperativity questions the possibility to limit the saturation of NSCP to one and the same site at stoichiometric amounts of calcium and protein as was done in an NMR study of NSCP (Prêcheur et al., 1996). The biological relevance of this binding mechanism is not clear as long as the exact biological role of these proteins is not known or limited to the concept of a calcium buffer.

The lifetime data on the R25D and R25D/D58R variants indicate that the salt bridge is present also in the apo

conformation of W57 and that orientation of the salt bridge is important to create the Ca^{2+}-like environment of W57. Recently it has been shown that the local electric field around the tryptophan residue can have a pronounced influence on the energy level of the low Trp ring-to-backbone charge transfer (Callis and Vivian, 2003) and the effect of Arg on the fluorescence might also be explainable by this effect. Quantum mechanical calculations are, however, necessary to confirm this.

Prof. C. Gielens is thanked for his help with the calcium determinations using the atomic absorption spectrophotometer. Myriam Moeyersons and Ine Vanopdenbosch are thanked for experimental support.

This project was supported by a research grant from the Fund for Scientific Research, G-00-92-01 (Flanders, Belgium), and a Concerted Research Action grant, GOA/2001/02.

REFERENCES

Alcala, J. R., E. Gratton, and F. G. Prendergast. 1987. Interpretation of fluorescence decays in proteins using continuous distributions. *Biophys. J.* 65:2313–2323.

Beechem, J. M., J. R. Knutson, J. B. A. Ross, B. W. Turner, and L. Brand. 1983. Global resolution of heterogeneous decay by phase modulation fluorometry: mixtures and proteins. *Biochemistry.* 22:6054–6058.

Bevington, P. R. 1969. Gradient-expansion algorithm. *In* Data Reduction and Error Analyses for the Physical Sciences. McGraw-Hill, New York. pp.235–240.

Burstein, E. A. 1983. The intrinsic luminescence of proteins is a method for studies of the fast structural dynamics. *Mol. Biol.* 17:455–467.

Burstein, E. A., and V. I. Emelyanenko. 1996. Log-normal description of fluorescence spectra of organic fluorophores. *Photochem. Photobiol.* 64:316–320.

Callis, P. R. 1997. ^1L_a and ^1L_b transitions of tryptophan: applications of theory and experimental observations to fluorescence of proteins. *Methods Enzymol.* 278:113–150.

Callis, P. R., and J. T. Vivian. 2003. Understanding the variable florescence quantum yield of tryptophan in proteins using QM-M simulations: quenching by charge transfer to the peptide backbone. *Chem. Phys. Lett.* 369:409–414.

Chang, A. C. Y., and S. N. Cohen. 1978. Construction and characterization of amplifiable multicopy DNA cloning vehicles from the P15A cryptic miniplasmid. *J. Bacteriol.* 1:1141–1156.

Chen, Y., and M. D. Barkley. 1998. Toward understanding tryptophan fluorescence in proteins. *Biochemistry.* 37:9976–9982.

Christiaens, B., S. Symoens, S. Verheyden, Y. Engelborghs, A. Joliot, A. Prochiantz, J. Vandekerckhove, M. Rosseneu, and B. Vanloo. 2002. Tryptophan fluorescence study of the interaction of penetratin peptides with model membranes. *Eur. J. Biochem.* 269:2918–2926.

Christova, P., J. A. Cox, and C. T. Craescu. 2000. Ion-induced conformational and stability changes in *Nereis* sarcoplasmic calcium binding protein: evidence that the Apo state is a molten globule. *Proteins.* 40: 177–184.

Clays, K., J. Jannes, Y. Engelborghs, and A. Persoons. 1989. Instrumental and analysis improvement in multifrequency phase fluorometry. *J. Phys. E Sci. Instrum.* 22:297–305.

Clark, P. L., Z. P. Liu, J. Zhang, and L. M. Gierach. 1996. Intrinsic tryptophans of CRABPI as probes of structure and folding. *Protein Sci.* 5:1108–1117.

Collins, J. H., J. A. Cox, and J. L. Theibert. 1988. Amino acid sequence of a sarcoplasmic calcium-binding protein from the sandworm *Nereis diversicolo*r. *J. Biol. Chem.* 263:15378–15385.

Cox, J. A., and E. A. Stein. 1981. Characterization of the new sarcoplasmic calcium binding protein with magnesium-induced cooperativity in the binding of calcium. *Biochemistry.* 20:5430–5436.

Craescu, C. T., B. Precheur, A. van Riel, H. Sakamoto, J. A. Cox, and Y. Engelborghs. 1998. H-1 and H-15 resonance assignment of the calcium-bound form of the *Nereis diversicolor* sarcoplasmic Ca^{2+}-binding protein. *J. Biomol. NMR.* 12:565–566.

Dahms, T. E. S., K. J. Willis, and A. G. Szabo. 1995. Conformational heterogeneity of tryptophan in a protein crystal. *J. Am. Chem. Soc.* 117:2321–2326.

Dekeyzer, N., Y. Engelborghs, and G. Volckaert. 1994. Cloning, expression and purification of a sarcoplasmic calcium-binding protein from the sandworm *Nereis diversicolor* via a fusion product with chloramphenicol acetyltransferase. *Protein Eng.* 7:125–130.

Desie, G., N. Boens, and F. C. De Schryver. 1986. Study of the time-resolved tryptophan fluorescence of crystalline a-chymotrypsin. *Biochemistry.* 25:8301–8308.

Durussel, I., Y. Luan-Rilliet, T. Petrova, T. Takagi, and J. A. Cox. 1993. Cation binding and conformation of tryptic fragments of *Nereis* sarcoplasmic calcium-binding protein: calcium-induced homo- and heterodimerization. *Biochemistry.* 32:2394–2400.

Eftink, M. R. 1990. Fluorescence techniques for studying protein structure. *Methods Biochem. Anal.* 35:117–129.

Engelborghs, Y., K. Mertens, K. Willaert, Y. Luan-Rilliet, and J. A. Cox. 1990. Kinetics of the conformational changes in Nereis sarcoplasmic calcium binding protein upon binding of divalent ions. *J. Biol. Chem.* 265:18809–18815.

Haiech, J., and M. C. Kilhoffer. 2000. Tryptophan calmodulin mutants. *In* Topics in Fluorescence Spectroscopy, Vol. 6: Protein Fluorescence. J. R. Lakowicz, editor. Kluwer Academic/Plenum Publishers, New York. pp.175–209.

Kirby, E. P., and R. F. S. Steiner. 1970. The influence of solvent and temperature upon the fluorescence of indole derivatives. *J. Phys. Chem.* 74:4480–4490.

Kretsinger, R. H., and C. E. Nockolds. 1973. Carp muscle calcium-binding protein. II. Structure determination and general description. *J. Biol. Chem.* 248:119–174.

Lakowicz, J. R., B. P. Maliwal, H. Cherek, and A. Balter. 1983. Rotational freedom of tryptophan residues in proteins and peptides. *Biochemistry.* 22:1741–1752.

Lakowicz, J. R., G. Laczko, and I. Gryczinski. 1985. 2-GHz frequency-domain fluorometer. *Rev. Sci. Instrum.* 57:2499–2506.

Lakowicz, J. R. 1999. Principles of Fluorescence Spectroscopy, 2nd Ed. Kluwer Academic/Plenum Publishers, New York. pp.329–330.

Lakowicz, J. R. 2000. On spectral relaxation in proteins. *Photochem. Photobiol.* 72:421–437.

Luan-Rilliet, Y., M. Milos, and J. A. Cox. 1992. Thermodynamics of cation binding to *Nereis* sarcoplasmic calcium-binding protein: direct binding studies, microcalorimetry and conformational changes. *Eur. J. Biochem.* 208:133–138.

Linse, S., C. Johansson, P. Brodin, T. Grundström, T. Drakenberg, and S. Forsén. 1991. Electrostatic contribution to the binding of Ca^{2+} in calbindin D_{9k}. *Biochemistry.* 30:154–162.

Lipari, G., and A. Szabo. 1980. Effect of librational motion on fluorescence depolarization and nuclear magnetic resonance relaxation in macromolecules and membranes. *Biophys. J.* 30:489–506.

Mach, H., C. R. Middaugh, and R. V. Lewis. 1992. Statistical determination of the average values of the extinction coefficients of tryptophan and tyrosine in native proteins. *Anal. Biochem.* 200:74–80.

More, J. J., and D. C. Sorensen. 1983. Computing a trust region step. *SIAM J. Sci. Stat. Comput.* 4:553–572.

Munier, H., A.-M. Gilles, P. Glaser, E. Krin, A. Danchin, R. Sarfati, and O. Bârzu. 1991. Isolation and characterization of catalytic and calmodulin-binding domains of *Bordetella pertussis* adanylate cyclase. *Eur. J. Biochem.* 196:469–474.

Nakayama, S., and R. H. Kretsinger. 1994. Evolution of the EF-hand family of proteins. *Annu. Rev. Biomol. Struct.* 23:473–507.

Parker, C. A., and W. T. Rees. 1960. Corrections of fluorescence spectra and the measurement of fluorescence quantum efficiency. *Analyst.* 85:587–600.

Permyakov, S. E., A. M. Cherskaya, I. I. Senin, A. A. Zargarov, S. V. Shulga-Morskoy, A. M. Alekseev, D. V. Zinchenko, V. M. Lipkin, P. P. Philippov, V. N. Uversky, and E. A. Peryakov. 2000. Effects of mutations in the calcium-binding site of recoverin on its calcium affinity: evidence for successive filling of the calcium binding sites. *Protein Eng.* 13: 783–790.

Prêcheur, B., J. A. Cox, T. Petrova, J. Mispelter, and C. T. Craescu. 1996. *Nereis* sarcoplasmic Ca^{2+} binding protein has a highly unstructured apo state which is switched to the native state upon binding the first Ca^{2+} ion. *FEBS Lett.* 395:89–94.

Raleigh, E. A., N. E. Murray, H. Revel, R. M. Blumenthal, D. Westaway, A. D. Reith, P. W. Rigby, J. Elhai, and D. Hanahan. 1988. McrA and McrB restriction phenotypes of some *E. coli* strains and implications for gene cloning. *Nucleic Acids Res.* 16:1563–1575.

Ross, J. A., C. J. Schmid, and L. Brand. 1981. Time-resolved fluorescence of the two tryptophans in horse liver alcohol dehydrogenase. *Biochemistry.* 20:4369–4377.

Ruggiero, A. J., D. C. Todd, and G. R. Fleming. 1990. Subpicosecond fluorescence anisotropy studies of tryptophan in water. *J. Am. Chem. Soc.* 112:1003–1014.

Sambrook, J., E. F. Fritsch, and T. Maniatis. 1989. Molecular Cloning: A Laboratory Manual, 2nd Ed. Cold Spring Harbor Laboratory, Cold Spring Harbor, New York.

Schoenmakers, T. J. 1992. CHELATOR: an improved method for computing metal ion concentrations in physiological solutions. *Biotechniques.* 12:870–879.

Sillen, A., and Y. Engelborghs. 1998. The correct use of ''average'' fluorescence parameters. *Photochem. Photobiol.* 67:475–486.

Sillen, A., J. Hennecke, D. Roethlisberger, R. Glockshuber, and Y. Engelborghs. 1999. Fluorescence quenching in the DsbA protein from *Escherichia coli*. The complete picture of the excited state energy pathway and evidence for the reshuffling dynamics of the microstates of tryptophan. *Proteins.* 37:253–263.

Sillen, A., J. F. Díaz, and Y. Engelborghs. 2000. A step toward the prediction of the fluorescence lifetimes of tryptophan residues in proteins based on structural and spectral data. *Prot. Sci.* 9:158–169.

Studier, F. W., and B. A. Moffat. 1986. Use of bacteriophage T7 RNA polymerase to direct selective high-level expression of cloned genes. *J. Mol. Biol.* 189:113–130.

Studier, F. W., A. H. Rosenberg, J. J. Dunn, and J. W. Dubendorf. 1990. Use of T7 polymerase to direct expression of cloned genes. *Methods Enzymol.* 185:60–89.

Tsien, R., and T. Pozzan. 1989. Measurement of cytosolic free Ca^{2+} with Quin 2. *Methods Enzymol.* 172:230–262.

Valeur, B., and G. Weber. 1977. Resolution of the fluorescence excitation spectrum of indole into the ^1L_a and ^1L_b excitation bands. *Photochem. Photobiol.* 25:441–444.

van Gilst, M., C. Tang, A. Roth, and B. Hudson. 1994. Quenching interaction and nonexponential decay: tryptophan 138 of bacteriophage T4 lysozyme. *J. Fluoresc.* 4:203–207.

van Riel, A. 1997. Karakterisatie van het Ca^{2+}-bindingsmechanisme van *Nereis* SCP met behulp van plaatsgerichte mutagenese. Katholieke Universiteit Leuven, Leuven, Belgium. (PhD thesis.)

Vijay-Kumar, S., and W. J. Cook. 1992. Structure of a sarcoplasmic calcium-binding protein from *Nereis diversicolor* refined at 2.0 Å resolution. *J. Biol. Chem.* 224:413–426.

Vivian, J. T., and P. R. Callis. 2001. Mechanisms of tryptophan fluorescence shifts in proteins. *Biophys. J.* 80:2093–2109.

Vos, R., R. Strobbe, and Y. Engelborghs. 1997. Gigahertz phase fluorometry using a fast high-gain photomultiplier. *J. Fluoresc.* 7:33S–35S.

Weber, G. 1977. Theory of differential phase fluorometry: detection of anisotropic molecular rotations. *J. Chem. Phys.* 66:4081–4091.

Weber, G. 1981. Resolution of the fluorescence lifetimes in a heterogeneous system by phase and modulation measurements. *J. Phys. Chem.* 85:949–953.

Willis, K. J., and A. G. Szabo. 1992. Conformation of parathyroid hormone: time-resolved fluorescence studies. *Biochemistry.* 31:8924–8931.